# Transport Coefficient and Heat Pulse Propagation in Tokamak Plasma

Yamaguchi, Hiroki
Interdisciplinary Graduate School of Engineering Sciences, Kyushu University

Yagi, Masatoshi
Research Institute for Applied Mechanics, Kyushu University

Ito, Sanae-I.
Research Institute for Applied Mechanics, Kyushu University

https://doi.org/10.5109/6786336

出版情報：Reports of Research Institute for Applied Mechanics. 41 (112), pp.53-76, 1995-09. 九州大学応用力学研究所

Reports of Research Institute for Applied Mechanics
Vol. XXXXI No. 112, 1995

# Transport Coefficient and Heat Pulse Propagation in Tokamak Plasma

By Hiroki YAMAGUCHI*, Masatoshi YAGI** and Sanae-I. ITOH**

Heat pulse propagation in Tokamak plasma is analyzed for various models of electron heat conduction coefficient $\chi_e$. Cases in which initial temperature perturbation induced by electron cyclotron heating (ECH) and sawtooth are studied. Five models are examined which have linear or nonlinear dependence on temperature or temperature gradient. The ratio ($\chi_{HP}/\chi_{PB}$) obtained from experiments shows more than 2, where $\chi_{HP}$ is the electron heat conductivity obtained from heat pulse propagation and $\chi_{PB}$ is that obtained from the stationary power balance. A model in which $\chi_e$ has a temperature gradient dependence could explain this ratio quantitatively. Also, $\chi_{HP}/\chi_{PB}$ is found to have appreciable radial dependence. Secondly, the problem of deducing $\chi_e$ from heat pulse propagation measurements is addressed. It is shown that simple diffusive models can not explain the experimental observations on WT-3 tokamak. The equation taking account of the convective term gives a good fit to experimental result.

***Contents***

I. Introduction ········· 54
II. Review ········· 55
III. What dependence must $\chi_e$ being consistent with experimental observations have?
  1. Basic equation and comparison conditions ········· 60
  2. Description of the initial temperature perturbation induced by sawtooth or electron cyclotron heating ········· 63
  3. Study of $\chi_{HP}/\chi_{PB}$ value for $\chi_e$ parameter dependence ········· 64
IV. Is heat pulse propagation really diffusive process?
  1. Model equation taking account of convective flux ········· 67
  2. Comparison study with the experimental observations in WT-3 tokamak ········· 68
  3. Re-examination of $\chi_e$ by an introduction of convective flux of heat pulse ········· 71
V. Summary and discussion ········· 73
References ········· 75

* Interdisciplinary Graduate School of Engineering Sciences, Kyushu University
**Research Institute for Applied Mechanics, Kyushu University

***Key words***: electron heat conduction coefficient, heat pulse, tokamak, sawtooth, electron cyclotron heating, plasma

## I. Introduction

Since the dominant transport losses in a tokamak are apparently produced by radial electron heat transport, it is of fundamental importance to experimentally measure the radial electron heat diffusivity coefficient. Experimentally, $\chi_e$ can be assessed by analyzing the spatial diffusion of a perturbation of the equilibrium profile of the electron temperature, $T_{eo}(r)$. The local perturbation $\tilde{T}_e(r)$ is measured as a function of time at various positions in the plasma simultaneously. The sudden change of the central part of the $T_{eo}(r)$ profile as a result of the sawtooth instability and the local electron perturbation induced by electron cyclotron heating (ECH) are used as initial perturbation. The radial diffusion of this perturbation is called heat pulse propagation. Studies of the propagation of heat pulses following sawtooth crashes and ECH started with the hope that this approach would yield a local measurement of the electron thermal diffusivity, independent of the uncertainties of power balance analysis, and which then might improve understanding of the nature of anomalous transport.[1][2]

When studies of sawtooth induced heat pulse propagation were undertaken, it was found that the thermal diffusivity, $\chi_{HP}$ derived by heat pulse propagation is, in many cases, much lager than the thermal diffusivity derived from power balance, $\chi_{PB}$.[3][4] Further, different perturbation analysis methods, used on same data, often give different answer. For the example discussed below, $\chi_{HP}$ is 6 $m^2/s$ using the simple time-to-peak method,[3][5] 12 $m^2/s$ with the extended time-to-peak method,[4] and 5 and 21 $m^2/s$, using the phase and amplitude Fourier-analysis methods,[3][6] respectively. In the region of interest the power-balance $\chi_{PB}$ was only 1.5 $m^2/s$.

It is a long-standing debate whether the difference between $\chi_{HP}$ and $\chi_{PB}$ is a genuine property of transport or an artifact introduced by the perturbation. It has been shown in the literature[7][8] that $\chi_{HP}$ can significantly exceed $\chi_{PB}$ if $\chi_{PB}$ is an increasing function of $\nabla T_e$, and that such a dependence is consistent with global confinement properties. It has also been in the literature[9][10] whether short-lived turbulence induced by the sawtooth instability itself could speed up the sawtooth heat pulse, and thus corrupt the determination of $\chi_{HP}$. This is normally referred to as "ballistic effect." A recent analysis of TFTR heat pulse data seems to indicate that the effect can not be the sole cause for the observed large discrepancy between $\chi_{HP}$ and $\chi_{PB}$.[11]

In heat pulse propagation study, it has been assumed that the $\chi_e$ value is constant and the evolution of heat pulse propagation is governed by diffusive process in all confinement region. We take a view that the course of discrepancy between $\chi_{HP}$ and $\chi_{PB}$ may exist in these assumptions.

The relevant form of the transport equations and the actual causes of the confinement degradation still remain an open guestion. With regard to the actual form of nonlinear dependence of $Q$ and $\nabla T_e$, it is not possible at present to discriminate between a highly nonlinear, on off-set linear or a critical gradient relation.[12]

In order to address these questions, we formulate next two issues : (1) whether the thermal conductivity being linear or non-linear dependence on the temperature or temperature gradient could explain this discrepancy, or not, and (2) whether the electron temperature perturbation equation including the convective term could explain experimental observations, or not. These are tested by numerical analysis.

This paper is organized as follows. In Chap. II, we review the method to obtain simple estimates of the $\chi_e$ value from the analysis of heat pulse propagation and experimental observations. The ratio of electron heat diffusivity $\chi_{HP}$ to $\chi_{PB}$ is considered. The experimental observations show that, basically, in all cases $\chi_{HP}$ is above the corresponding $\chi_{PB}$ typically by a factor of 3. In Chap. III, we discuss the question whether the thermal conductivity has a linear or non-linear dependence on the temperature or temperature gradient. Numerical model equation of heat pulse propagation is solved. It is consequently shown that $\chi_e$ having a dependence on the temperature gradient ($\chi_e \propto \nabla T$, $(\nabla T)^{3/2}$) is not inconsistent with the most experiment results ($\chi_{HP}/\chi_{PB} \geqq 2$). In Chap. IV, we discuss whether heat pulse propagation is diffusive process. Comparison study of the experimental observations with the simulations is done. It is found that simple diffusive models can not explain the experimental observations on WT-3 tokamak. It is also indicated the model equation taking account for the convective term gives a good fit to experimental results. Finally, summary and discussion are presented in Chap. V.

## II. Review

The main feature of electron heat transport taking place when internal disruptions appear are the following. At a certain instant of time during the discharge, the balance between sources of heat (Ohmic heating, neutral injection, etc.) and sinks (radiation, internal conversion, etc.) which resulted in a certain steady temperature profile $T_e(r)$ for the plasma column, is abruptly flattened out to a certain radius, $r_0$. Because of the formation of a magnetic island with a time scale much faster than the phenomena of normal heat diffusion, the electron heat diffusion coefficient $\chi_e(r)$ becomes practically infinite from $r=0$ to $r=r_0$, where $r_0 \simeq \sqrt{2} r_s$, $r_s$ being the singular surface $q=1$. This results in a practically flat temperature profile throughout the mentioned range as shown in Fig. 1, so that the central temperature is lowered from $r=0$ to $r=r_s$ and increased from $r=r_s$ to $r=r_0$ at a certain instant of time ; the net or total heat content is unchanged (Fig. 1).[3]

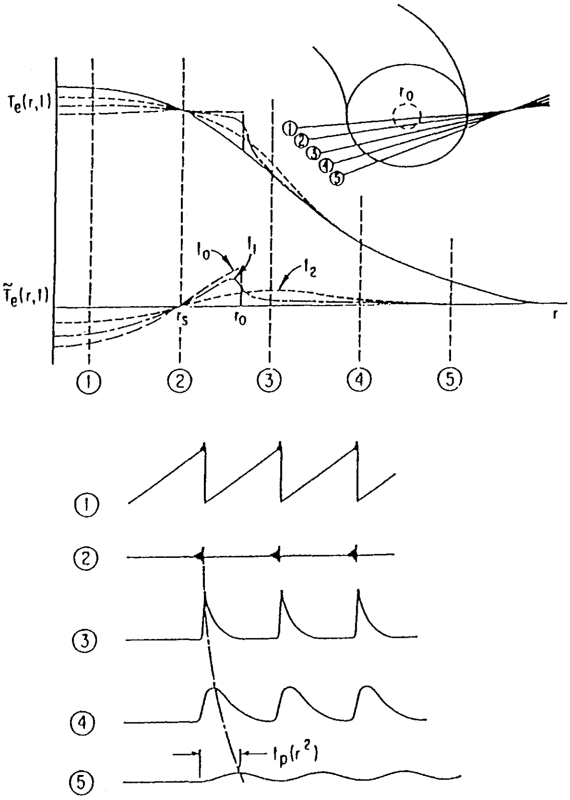


Fig. 1 Schematic illustration of soft-X-ray diagnostic chords and the evolution of the electron temperature perturbation $T(r, t)$ as a function of time. The signals below indicate the temporal variation of the soft-X-ray signals from the various chords (1-5). At later times $t_2 > t_1 > t_0$ the sawtooth induced heat pulse diffuses outwards from the radius $r_o$ to which reconnection (flattening of $T_e$) takes place. (cited from Ref. [16], Fig. 1)

The resulting heat profile provides the initial condition for our problem with the points $r = r_s$ dividing regions of opposite phase in the heat perturbation. The phase starts downward inside $r = r_s$ and upward outside.

The determination of the equilibrium state through a precise knowledge of the amount of radiation, current profile, etc. will no longer be our concern. Instead, our subject will be the perturbation of this state with an equilibrium temperature profile $T_e(r)$ which can be experimentally observed.[5)]

Let us start with the general equation determining the electron temperature

$$\frac{3}{2}\frac{\partial n_e T_e(r,\ t)}{\partial t}=\frac{1}{r}\frac{\partial}{\partial r}\left[rn_e\chi_e\frac{\partial T_e(r,\ t)}{\partial r}\right]+\eta J^2+\Sigma Q \tag{2-1}$$

where $\eta J^2$ represents Ohmic heating, and $\Sigma Q$ represents other sources and sinks such as injection, radiation, recombination, etc. (We shall suppress the subscript in $T_e$ and $n_e$, for simplicity.)

We shall call $T_0(r)$ the equilibrium temperature profile just before disruption. Clearly, it is determined by

$$\frac{1}{r}\frac{\partial}{\partial r}\left[rn\chi\frac{\partial T_0(r)}{\partial r}\right]+\eta J^2+\Sigma Q=0 \tag{2-2}$$

Suppose now a disruption takes place at time $t=0$, leaving the system in the state $T(r,\ 0)$ (Fig. 1). The evolution from this state $T(r,\ 0)$ at later times would be described by $T(r,\ t)$, which is governed by Eq. (2-1) subject to the initial condition $T(r,\ t)=T(r,\ 0)$ at $t=0$.

Rather than studying $T(r,\ t)$, we shall study the evolution of the perturbation $\tilde{T}(r,\ t)=T(r,\ t)-T_0(r)$, which obviously satisfies the much simpler equation

$$\frac{3}{2}n\frac{\partial\tilde{T}(r,\ t)}{\partial t}=\frac{1}{r}\frac{\partial}{\partial r}\left[rn\chi\frac{\partial\tilde{T}(r,\ t)}{\partial r}\right] \tag{2-3}$$

and is subject to the initial condition

$$\tilde{T}(r,\ 0)=T(r,\ 0)-T_0(r),\ t=0 \tag{2-4}$$

The shape of $\tilde{T}(r,\ 0)$ is shown in Fig. 1.

In obtaining Eq. (2-3), we have implicitly assumed that the source terms and, in particular, $\eta J^2$ do not appreciably change during the disruptive process. This is justified on two grounds. In the first place, it is easy to see that the source terms is Eq. (2-3) are of the same magnitude as the corresponding ones in Eq. (2-1), whereas the perturbed-source term which has been omitted from Eq. (2-3) is smaller by $\tilde{T}/T$, assuming constant $J$ and Spitzer resistivity. And, secondly, it can be shown numerically that the relative change in $\eta J^2$ does not amount to more than 3% because of changes in $J$. We are also neglecting the magnetic contribution to the kinetic energy which is released at disruption and is indicated by a large but very localized induced-voltage spike outside $r_0$ that rapidly diffuses away, since the energy change is less than 10% for the typical cases considered (This is warranted both by numerical calculations of the disruptive process as in the reference,[13] and by direct calculation using Kadomtsev's modelling.[14]).

Our task will be to extract as much information as possible on $\chi(r)$ from the experimental measurement of $T(r,\ t)$. Eventually, of course, this information should be fed into Eq. (2-1) so as to help to determine the proper profiles of the sources and sinks.

Before we try to determine $\chi(r)$, we should show that Eqs. (2-3) and (2-4) indeed reproduce the experimental observed diffusive temperature perturbation profiles. To do this, we shall work out an approximate solution to Eqs. (2-3) and

(2-4), assuming that, at least for radii not too large, the density $n$ and the coefficient $\chi$ can be taken as constant. Formally, one has in this case

$$\tilde{T}(r,\ t)=\frac{a^2}{4\pi}\int_V \tilde{T}(r',\ 0)G_{t'=0}dV$$

$$a^2=\frac{3}{2\chi} \tag{2-5}$$

$G_{t'=0}$ represents the Green's function at time $t=0$ in cylindrical co-ordinates, $dV$ the volume element, and the integration is extended over the whole space.

The general form of $\boldsymbol{G}$ is

$$G(\vec{r}-\vec{r}',\ t-t')=\frac{1}{t-t'}\exp\left(-\frac{a^2}{4(t-t')}|\vec{r}-\vec{r}'|^2\right)\theta(t-t')$$

where $\theta(t-t')$ stands for the Heaviside step function, and $\vec{r}$, $\vec{r}'$ represent vectors. Since $|\vec{r}-\vec{r}'|^2=r^2+r'^2-2rr'\cos\theta$, the angular integration can be carried out in Eq. (2-5), according to

$$\int_0^{2\pi} d\theta\exp(a^2rr'\cos\theta/2t)=2\pi I_0\left(\frac{a^2rr'}{2t}\right) \tag{2-6}$$

where $I_0$ is the modified Bessel function. So, finally, we have

$$\tilde{T}(r,\ t)=\frac{a^2}{2t}\exp(-a^2r^2/4t)$$

$$\int_0^\infty r'dr'\tilde{T}(r',\ 0)\exp(-a^2r'^2/4t)I_0\left(\frac{a^2rr'}{2t}\right) \tag{2-7}$$

A brief description will now be given of a method for measuring $\chi$ based on observation of the time of arrival $t_p$ of the peak of the heat pulses as they are observed from different radii. A more complete discussion can be found in the reference.[2] This method has historical interest since it was the first to be used for determining $\chi$ from heat pulse propagation.[1)2)] For reasons that will become clear, the $\chi$-value obtained appeared much higher than expected from rough energy-containment-time calculations.

If we look at the behavior of $\tilde{T}(r,\ t)$ in the simple dipole approximation

$$\int_0^{r_0} r'\tilde{T}(r',\ 0)dr'=r_1r_sT_-+(r_0-r_s)r_2T_+ \tag{2-8}$$

where $r_1$ and $r_2$ are defined as $0<r_1<r_s$ and $r_s<r_2<r_0$, respectively. For Eq. (2-7) at large t, we may approximate the Bessel function by the small parameter expansion. This gives

$$\tilde{T}(r,\ t)\simeq\frac{a^6Ar^2}{32}\frac{1}{t^3}\exp(-a^2r^2/4t),\ A=r_1r_sT_- \tag{2-9}$$

The maximum of $\tilde{T}(r,\ t)$ lies at

$$\frac{\partial\tilde{T}}{\partial t}\sim\left(-\frac{3}{t^4}+\frac{a^2r^2}{4t^5}\right)\exp(-a^2r^2/4t)=0 \tag{2-10}$$

so

$$\chi=\frac{r^2}{8t_p} \tag{2-11}$$

If we plot the experimental time delay $(t_p)$ of arrival of the heat pulse peak at differential radii $(r)$ versus $r^2$, the observed slope should be a straight line giving directly $\chi$ for large values of $r^2$. This method obtaining $\chi_e$-values is called simple time-to-peak method.

We define that $\chi_{HP}$ and $\chi_{PB}$ are thermal diffusivity derived by heat pulse propagation and that derived from power balance, respectively. No good agreement is obtained between $\chi_{HP}$ and $\chi_{PB}$ if the analysis is done on the basis of a simple diffusive model.[15] Basically, in all cases $\chi_{HP}$ is above the corresponding $\chi_{PB}$ typically by a factor of 3 (see Table 1).

The largest discrepancy is obtained in TFTR with factors >10.[16] The discrepancy between steady state $\chi_{PB}$ and dynamic $\chi_{HP}$ heat diffusivity in tokamaks may have several causes and gives rise to various interpretations. The most obvious one, that the sawtooth event introduces perturbed plasma condi-

Table 1 Ratio of electron heat diffusivity $\chi_{HP}$ as measured by ECRH modulation or by sawtooth (sth) propagation to $\chi_{PB}$ as deduced from standard power balance analysis for various experiments. (cited from Ref. | 23 | , Table 1)

| Experiment | $\chi_e^{hp}/\chi_e^{pb}$ | Reference | |
|---|---|---|---|
| ASDEX | 3 | (sth) | Giannone *et al* 1990 |
| DIII-D | ≈1 | (ECRH) | Lopes Cardozo *et al* 1992b |
| DITE | ≈1 | (ECRH) | Hugill *et al* 1988 |
| FTU | 1.5-2.2 | (sth) | Alladio *et al* 1992b |
| ISX-B | ≈1 | (sth) | Bell *et al* 1984 |
| JET | 2.5 | (sth) | Tubbing *et al* 1987 |
| JT-60U | 2-4 | (sth) | de Haas *et al* 1992 |
| RTP | 2-4 | (sth) | Lopes Cardozo *et al* 1992a |
| RTP | 2-4 | (ECRH) | Lopes Cardozo *et al* 1992a |
| TEXT | 2.25 | (sth) | Brower *et al* 1990 |
| TEXTOR | >4 | (sth) | Krämer-Flecken, private communication |
| TFTR | 1−>10 | (sth) | Fredrickson *et al* 1986 |
| TORE SUPRA | 2.5-3.5 | (sth) | Lopes Cardozo *et al* 1992b |
| T10 | ≈1 | (sth) | Sillen *et al* 1986 |
| W7-AS | 1-1.5 | (ECHR) | Giannone *et al* 1991 |

tions for the heat wave measurement, may be ruled out by the confirmation of the discrepancy between $\chi_{HP}$ and $\chi_{PB}$ by ECRH heat modulation studies, too, as observed on, for example, RTP[17] and WT-3[18]. Another discrepancy between the two $\chi_e$ values is the lack of parameter dependence of $\chi_{HP}$. In the case of JET, $\chi_{HP}$ is independent of $I_p$, $P$ and $\bar{n}_e$ and is the same for OH, L- and H-mode plasma in spite of the distinct differences in confinement and plasma profiles in these various regimes.[19]

Only the above mentioned onset or nonlinear relations allow an understanding of the discrepancy between $\chi_{HP}$ and $\chi_{PB}$ and the weak, or even lack of, power dependence of $\chi_{HP}$. The response times for tokamak transport changes seem to be fast enough so that non-linearities or critical gradient effects can come to bear during the short time scales of heat wave propagation.[20]

The relevant form of the transport equations and the actual causes of the confinement degradation still remain an open question. There is strong evidence that both heat and particle fluxes have dependences, as sketched in Fig. 2.[21] With regard to the actual form of nonlinear dependence of $Q$ and $\nabla T_e$, it is not possible at present to discriminate between a highly nonlinear[22], on off-set linear or a critical gradient relation (see Fig. 2).[12]

The difference between particle and energy transport could be that in particle transport the strong non-linearities are introduced by a large off diagonal element balancing a large diffusive term. But the diffusive term may have a rather linear dependence on its driving force. Heat transport, on the other hand, may have small off diagonal contributions but a strong nonlinear dependence of its flux on the conjugate force.[23]

## III. What dependence must $\chi_e$ being consistent with experimental observations have ?

### 1. Basic equation and comparison conditions

Any theory invoked to explain anomalous transport have not been developed. And numerical simulations based on models for the heat transport have been compared with the experimental data in order to gain a deeper insight into the nature. Here, we pay attention to the dependence on temperature or temperature gradient about model theories. We choose various $\chi$ models, i.e. $\chi \propto T$ (Bohm type), $\chi \propto T^{3/2}$ (Gyro Bohm type), $\chi \propto \nabla T$ (Rebut-Lallia-Watkins model), $\chi \propto (\nabla T)^{3/2}$ (Itoh's model) and $\chi \propto T^0$ (constant coefficient).

Starting from the analysis on the stationary power balance profile, evolution of the temperature perturbation by use of heat propagation analysis is examined. We compare values of $\chi_{HP}/\chi_{PB}$ for each electron conductivity, because the $\chi_e$-values derived from heat pulse propagation ($\chi_{HP}$) differ from those obtained from the stationary power balance ($\chi_{PB}$) in the experiments.

In this chapter, the proposal that thermal conductivity having linear or non-linear dependence on the temperature or temperature gradient could explain this discrepancy is tested. Numerical modeling of heat pulse propagation is

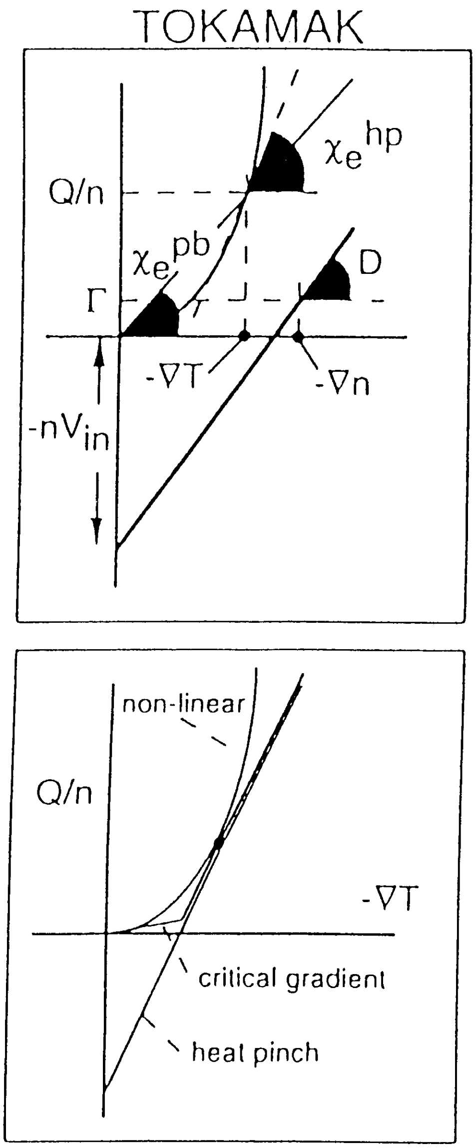


Fig. 2 Schematics which indicate the possible relationships between heat flux $Q/n$ and $-\nabla T$ and particle flux $\Gamma$ and $\nabla n$ for tokamaks. The hard facts ($\chi_{HP} \neq \chi_{PB}$) are indicated. The nonlinear relation between $Q/n$ and $-\nabla T$ could described by a heat pinch or a critical gradient model. (cited from Ref. [23], Fig. 13)

solved as a forced boundary value problem.

Following the work of Soler and Callen,[5] a mathematical description of the heat pulse propagation problem is provided, beginning from the general electron heat balance equation:

$$\frac{3}{2}\cdot\frac{\partial n_e\cdot T_e(r,\ t)}{\partial t}=\frac{1}{r}\cdot\frac{\partial}{\partial r}\left[r\cdot n_e\cdot\chi_e(r,\ t)\cdot\frac{\partial T_e(r,\ t)}{\partial r}\right]+\Sigma Q \tag{3-1}$$

where $n_e$ is the electron density; $T_e$ is the electron temperature; $\chi_e$ is the electron conductivity; $\Sigma Q$ represents all electron heat sources and sinks, such as Ohmic heating, collisional heat transfer to ions, convection, radiation and auxiliary heating.

A small electron temperature perturbation $\tilde{T}(r,\ t)$ of a near-equilibrium situation is governed by the equation:

$$\frac{3}{2}\cdot n_e\cdot\frac{\partial\tilde{T}(r,\ t)}{\partial t}=\frac{1}{r}\cdot\frac{\partial}{\partial r}\left[r\cdot n_e\cdot\chi_e\cdot\frac{\partial\tilde{T}(r,\ t)}{\partial r}\right]+\frac{1}{r}\cdot\frac{\partial}{\partial r}\left[r\cdot n_e\cdot\tilde{\chi}(r,\ t)\cdot\frac{\partial T_{e0}(r,\ t)}{\partial r}\right] \tag{3-2}$$

This equation is derived by perturbing Eq. (3-1) and neglecting the additional term $\tilde{T}\cdot\frac{\partial\Sigma Q}{\partial T}\sim-\frac{n\cdot\tilde{T}}{\tau_E}$ because the equilibrium evolution implied by this term is slow and broadly distributed to relative to the highly localized (in space and time) perturbations $\tilde{T}(r,\ t)$ induced by the electron cyclotron resonance heating (ECH) or sawtooth crashes. Equation (3-2) indicates that heat pulse is explicitly affected by stationary power balance profile as a background. That is different from the previous works subjecting to the constant $\chi_e$ condition.

We hypothesize $\chi_e$ has a dependence on temperature or temperature gradient, i.e.

$$\chi_e=Const,\ \alpha T,\ \beta|\nabla T|,\ \gamma T^{3/2},\ \delta|(\nabla T)^{3/2}|$$

where $\alpha$, $\beta$, $\gamma$, $\delta$ are proportional constants. And we examine the different effect on heat pulse propagation due to the difference of the various dependence of $\chi_e$. At first, as preparing to compare the various dependence on temperature or temperature gradient in $\chi_e$, we solve the stationary power balance profile and determine the values of the proportional constant for each $\chi_e$ respectively. To be concrete, we set $\frac{\partial T_e(r,\ t)}{\partial t}$ term to zero in Eq. (3-1). And the primary assumptions are that the electron density $n_e$ and all electron heat sources and sinks $\Sigma Q$ are constant in radius. Furthermore, for the comparison study, we impose that:

(1) The boundary conditions are that

$$T_{e0}=0\ (r=a),\ \frac{\partial T_{e0}}{\partial r}=0\ (r=0)$$

in which, $a$ is the plasma radius.

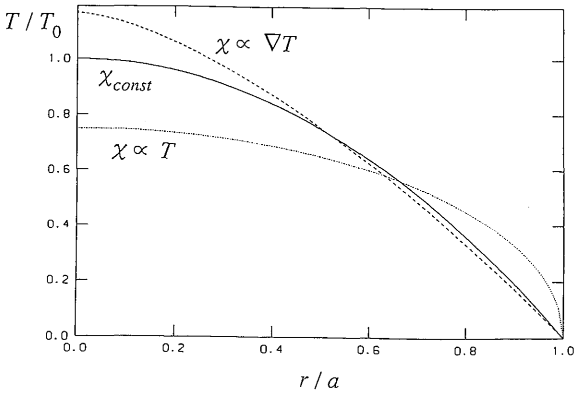


Fig. 3 The stationary power balance profiles for $\chi_{const}$ $\chi \propto T$, $\chi \propto \nabla T$. $T_0$ is the central temperature for the constant heat conductivity.

Table 2 The values of the proportional constants for $\chi_e$.

| $\chi_{const}$ | $\alpha$ | $\beta$ | $\gamma$ | $\delta$ |
|---|---|---|---|---|
| 1.000 | 14.22 | 2.612 | 48.78 | 4.246 |

(2) The internal energy $W_p\left(\equiv \int_{r=0}^{r=a} n_e \cdot T_{e0} \cdot dV\right)$ for each $\chi_e$ takes the same value.

Imposing above conditions, we simultaneously determine the stationary profiles and the values of the proportional constants, respectively. These are shown in Fig. 3 and Table 2. Figure 3 indicates that the profile for $\chi \propto T$ tends to have the larger temperature gradient near the edge (low temperature), on the contrary, the profile for $\chi \propto \nabla T$ tends to make the temperature gradient uniform. The reason that the temperature for $\chi \propto \nabla T$ is higher than that for $\chi \propto T$ at the center of the plasma is the assumption that the temperature at edge is zero. If the temperature at the edge is higher than a certain value, it is reversed.

## 2. Description of the initial temperature perturbation induced by sawtooth or electron cyclotron heating

We consider that initial temperature perturbation is induced by local electron heating due to electron cyclotron heating (ECH) or sawtooth crashes. ECH produces a localized heat perturbation and a well-defined heat pulse propagates outward. Hence we assume that initial condition of temperature perturbation induced by ECH is Gaussian distribution, i.e.

$$\tilde{T}_e(r,\ 0)=A\cdot\exp(-B\cdot(r-r_a)^2)$$

where A and B are parameter, $r_a$ is the peak of Gaussian distribution for the perturbation.

In the experiments, the ECH could produce a bi-Maxwellian initial distribution since it has the effect of mixing hot and cold components near the local ECH radius ($r_a$). Hence, the electron distribution may not be Maxwellian in the energy range of interest. But, we assume that electron distribution is Maxwellian, because the time scale of interest (0.1 msec < t < 1 msec) appears longer than the energy relaxation time at these energies [$\tau_{ee}/2\sim30$-$50\ \mu$sec].[1)]

On the other hand, sawtooth crash perturbs the temperature equilibrium profile $T_{e0}(r)$. The resulting temperature profiles are flat from the center to a certain radius $r_m$ ($r_m$ is called the mixing radius). Hence, initial condition of temperature perturbation induced by sawtooth crash is

$$\tilde{T}_e(r,\ 0)=T_{e0}(r_s)-T_{e0}(r)$$

where $r_s$ ($r_s$ is called the radius of disruption or the inversion radius.) is the radius where the temperature should show no change. As a result of sawtooth crash, the central temperature is lowered from $r=0$ to $r=r_s$ and increased from $r=r_s$ to $r=r_m$ at a certain instant of time. The net or total heat content is unchanged. Hence, $\tilde{T}_e(r,\ 0)$ must meet the following qualification,

$$\int_0^{r_m} r'\cdot\tilde{T}_e(r',\ 0)\cdot dr'=0$$

This condition determines the value of $r_m$ for a certain value of $r_s$ and the initial temperature perturbation $\tilde{T}_e(r,\ 0)$ numerically. In the numerical analysis, we modify the obtained $\tilde{T}_e$ shape smooth near $r=r_m$ evading divergence of $\nabla\tilde{T}_e$ at $r=r_m$.

We are also interested in the variation of $\chi_e$ associated with the perturbation of temperature. Figure 4 shows that the value of the heat conductivity vs. plasma radius in case that initial temperature perturbation is induced by ECH. The value of $\chi_e$ in proportion to temperature gradient are influenced remarkably by the perturbation of temperature in contrast to that in proportion to temperature. It is shown that the value of $\chi_e$ having temperature gradient dependence is reduced inside the heat pulse and increased outside that. This characteristic enhancement of $\chi_e$ may cause the discrepancy between the value of $\chi_{HP}$ and that of $\chi_{PB}$.

## 3. Study of $\chi_{HP}/\chi_{PB}$ value for $\chi_e$ parameter dependence

The variation of the heat flux associated with the perturbation of the tempetature is calculated from the various assumption for the heat conductivity. Writing $T=T_0+\tilde{T}$ and heat flux.

$$q=q_0+\tilde{q} \qquad (3\text{-}3)$$

we define $\chi_{HP}$, $\chi_{PB}$ respectively,

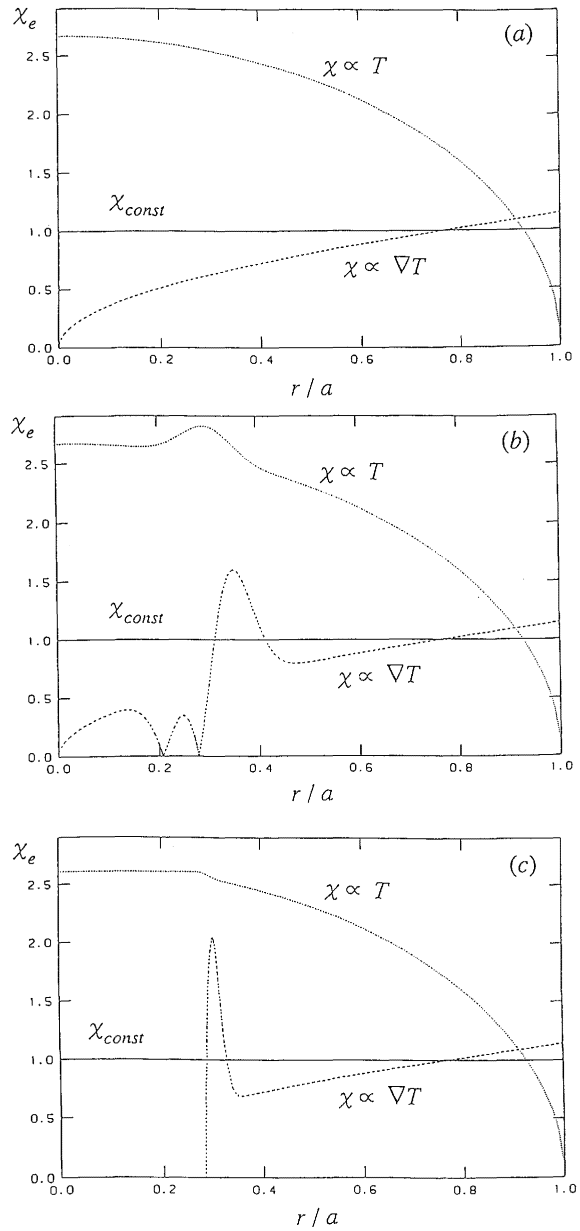


Fig. 4 The value of heat conductivity having temperature or temperature gradient dependence is influenced by the initial perturbation. Figure 4 represents that heat conductivity vs. plasma radius in case of the stationary power balance (a), the auxiliary heating (ECH) as a initial perturbation added to the stationary power balance (b) and sawtooth (c).

$$q_0 = -n_e \cdot \chi_{PB} \cdot \nabla T_0 \tag{3-4}$$

$$\tilde{q} = -n_e \cdot \chi_{HP} \cdot \nabla \tilde{T} \tag{3-5}$$

If we write $\chi = \chi_0 + \tilde{\chi}$, we have

$$\begin{aligned} q &= -n_e \cdot \chi \cdot \nabla T \\ &= -n_e \cdot \chi_0 \cdot \nabla T_0 - n_e \cdot \left( \tilde{\chi} \cdot \frac{\nabla T_0}{\nabla \tilde{T}} + \chi \right) \cdot \nabla \tilde{T} \end{aligned} \tag{3-6}$$

Comparing Eqs. (3-3)-(3-6) lead to

$$\chi_{PB} = \chi_0 \tag{3-7}$$

$$\chi_{HP} = \chi_0 + \tilde{\chi} \cdot \left( 1 + \frac{\nabla T_0}{\nabla \tilde{T}} \right) \tag{3-8}$$

Using the Eqs. (3-7) and (3-8) and the stationary profile according to the model and the initial perturbation induced by ECH or sawtooth, we calculate the value of $\chi_{HP}/\chi_{PB}$ for the various models of heat conductivity. Table 3 shows the value of $\chi_{HP}/\chi_{PB}$ in case of that the initial temperature perturbation is induced by ECH (for parameters, $A = 0.1 \cdot T_0$, $B = 200/a^2$, $T_0$ is the central temperature in tokamak plasma and $a$ is the plasma radius.). Table 4 shows the value of $\chi_{HP}/\chi_{PB}$ in case of that the initial temperature perturbation is induced by sawtooth (for parameter, $r_s = 0.2 \cdot a$). The values of $\chi_{HP}/\chi_{PB}$ in the Table 3 and 4 are those in the case of $\frac{\partial \tilde{T}(r, t)}{\partial t} = 0$ at the radius. Hence, we can directly compare the value of $\chi_{HP}/\chi_{PB}$ in Tables 3 and 4 with those estimated by relation of peak arrival time and radial position in the experiments. Both Table 3 and Table 4 show $\chi_e$ having a dependence on the temperature gradient is not inconsistent with values of $\chi_{HP}/\chi_{PB}$ obtained from experiments. Since most experiment indicates that values of $\chi_{HP}$ a factor of 2 greater than $\chi_{PB}$ are obtained. Also

Table 3 The value of $\chi_{HP}/\chi_{PB}$ in case that initial temperature perturbation is induced by ECH.

| | $r/a=0.4$ | $r/a=0.5$ | $r/a=0.6$ |
|---|---|---|---|
| $\chi = const$ | 1.00 | 1.00 | 1.00 |
| $\chi = \alpha T$ | 1.04 | 1.02 | 1.01 |
| $\chi = \gamma T^{3/2}$ | 1.06 | 1.03 | 1.02 |
| $\chi = \beta \mid \nabla T \mid$ | 2.28 | 2.06 | 2.02 |
| $\chi = \delta \mid \nabla T^{3/2} \mid$ | 3.01 | 2.61 | 2.54 |

Table 4 The value of $\chi_{HP}/\chi_{PB}$ in case that initial temperature perturbation is induced by sawtooth.

| | $r/a=0.4$ | $r/a=0.5$ | $r/a=0.6$ |
|---|---|---|---|
| $\chi=const$ | 1.00 | 1.00 | 1.00 |
| $\chi=\alpha T$ | 1.00 | 1.00 | 1.00 |
| $\chi=\gamma T^{3/2}$ | 1.00 | 1.00 | 1.00 |
| $\chi=\beta \mid \nabla T \mid$ | 2.07 | 2.02 | 2.01 |
| $\chi=\delta \mid \nabla T^{3/2} \mid$ | 2.63 | 2.53 | 2.51 |

seen is that the radial dependence of $\chi_{HP}/\chi_{PB}$ for $\chi_e$ having a dependence on the temoperature gradient is influenced by the initial perturbation profile. In particular, the values of $\chi_{HP}/\chi_{PB}$ increase near the perturbation radius. However, the enhancement is suppressed in the simulated sawtooth case as seen from Tables 3 and 4.

## Ⅳ. Is heat pulse propagation really diffusive process ?

### 1. Model equation taking account of convective flux

A mathematical description of the heat pulse propagation problem is provided, beginning from the general electron equation determining the electron temperature :

$$\frac{3}{2}\cdot\frac{\partial n_e\cdot T_e(r,t)}{\partial t}+\frac{3}{2}\cdot\bar{v}_r\cdot\frac{\partial n_e\cdot T_e(r,t)}{\partial r}=\frac{1}{r}\cdot\frac{\partial}{\partial r}\left[r\cdot n_e\cdot\chi_e\cdot\frac{\partial T_e(r,t)}{\partial r}\right]+\Sigma Q \qquad (4\text{-}1)$$

where $n_e$ is the electron density ; $T_e$ is the electron temperature ; $\chi_e$ is the electron conductivity ; $\bar{v}_r$ is the convective velocity ; $\Sigma Q$ represents all electron heat sources and sinks.

A small electron temperature perturbation $\tilde{T}(r, t)$ of a near-equilibrium state may be governed by the equation :

$$\frac{3}{2}\cdot n_e\cdot\frac{\partial\tilde{T}(r,t)}{\partial t}+\frac{3}{2}\cdot n_e\cdot\bar{v}_r\cdot\frac{\partial\tilde{T}(r,t)}{\partial r}=\frac{1}{r}\cdot\frac{\partial}{\partial r}\left[r\cdot n_e\cdot\chi_e\cdot\frac{\partial\tilde{T}(r,t)}{\partial r}\right]$$

$$+\frac{1}{r}\cdot\frac{\partial}{\partial r}\left[r\cdot n_e\cdot\tilde{\chi}\cdot\frac{\partial T_{e0}(r)}{\partial r}\right]-\frac{1}{\tau_d}\cdot n_e\cdot\tilde{T}(r,t) \qquad (4\text{-}2)$$

and is subject to the initial condition

$$\tilde{T}_e(r,0)=T_e(r,0)-T_{e0}(r),\ t=0. \qquad (4\text{-}3)$$

Here, $T_{e0}(r)$ is the equilibrium temperature profile just before the initial perturbation induced by ECH or sawtooth crash. $\Sigma Q$ has been linearized in $T_e$ with the help of a characteristic damping time constant,[4] $\tau_d=-n_e\cdot(\partial\Sigma Q/\partial T_e)^{-1}$. We write $\chi_e=\chi_0+\tilde{\chi}$ because we may take account of the case where $\chi_e$ has a dependence on temperature or temperature gradient. The models in which $v_r=0$ and $\tau_d \to \infty$ are assumed are called as diffusive models and the models in which $v_r=0$ is assumed are called as extended diffusive models. As was demonstrated by Goedheer,[24] neglecting the damping term is not always allowed and can lead to an overestimate of $\chi_e$ by up to a factor of two. Following Goedheer,[24] for $\tilde{T}_i \ll \tilde{T}_e$, $\tau_d$ can be expressed as

$$\tau_d^{-1}=\frac{3}{2}\left(\frac{3T_i}{T_{e0}}-1\right)\frac{m_e}{m_i\tau_{ei}}+\frac{3}{2}\frac{\eta j^2}{n_e T_{e0}}+\frac{1}{n_e}\frac{\partial P_{rad}}{\partial T_{e0}}. \tag{4-4}$$

The three terms are the contributions of electron-ion energy exchange, the Ohmic dissipation and the radiative losses, respectively. Which term dominates depends on the plasma parameters and, therefore, also on radial position. As is clear from Eq. (4-2), the damping is important if $\tau_d \leq \lambda^2/\chi_e$, where $\lambda$ denotes the typical scale-length of the $T_e$ profile perturbation. Typically, $\lambda \approx a/3$ ($a$ denoting the plasma radius),[4] so that damping plays a role when $K \equiv a^2/(\tau_d \chi_e) \geq 10$. But in smaller machines, the damping effect is generally less by using the well known relation $\tau_d \approx a^2/(4\chi_e)$ for the energy confinement time,[7] $K$ can be estimated by $K \approx 4\tau_e/\tau_d$, which is often very small.

## 2. Comparison study with the experimental observations in WT-3 tokamak

We analyze the data obtained from WT-3 tokamak experiments.[25] In the experiments, major and minor radii are R = 65cm and a = 20cm, respectively. The toroidal field was $B_T \leq 1.75T$, and the plasma current was $I_P \leq 150kA$. The typical electron temperature at the plasma center was $T_e \simeq 0.3keV$ (measured with Thomson scattering), and the line averaged electron density was $\bar{n}_e=0.4-0.8\times10^{13}\ cm^{-3}$ at the center of plasma. The sharply focused microwave from a gyrotron ($\omega/2\pi=56GH_z$, $P_{EC}\leq 200kW$) is absorbed at the secondharmonic ECH resonance layer, $R_{2\Omega e}$ and produces a local heat pulse around $R_{2\Omega e}$. In this paper, $R_{2\Omega e}$ is located on the magnetic axis at any time.

The temperature perturbation profiles at the end of each ECH pulse are shown in Fig. 5 (a), (b) and (c). These are corresponding to 0.3 ms (a), 0.5 ms (b) and 0.8 ms (c) in ECH pulse length, respectively. The data points are approximately on Gaussian distribution obtained by using the least squares fit. It is plotted in Fig. 6 that the experimental time delay ($t_p$) of arrival of the heat pulse peak at differential radii ($r$) versus $r^2$ corresponding to 0.3 ms (a), 0.5 ms (b) and 0.8 ms (c) in ECH pulse length in Fig. 5.[25]

For determining the value of $\chi_e$, we use the simple time-to-peak method. The simple time-to-peak method is derived from assuming $\chi_e$ const, $v_r=0$ and $\tau_d \to \infty$ in Eq. (4-2). In this experiment, $\tau_d \to \infty$ is permitted because $K \approx 2$ is obtained by taking $a=0.2m$, $\chi_e \approx 1m^2/s$ and $\tau_{ei} \approx 25ms$ as a rough estimate for $\tau_d$. If the above assumptions are permitted, from the relation $\chi_{HP}=\frac{3}{8}\frac{(\Delta r)^2}{t_p}$, we roughly estimate the electron diffusivity as $\chi_{HP}=2.22\pm0.52m^2/s$, $3.00\pm1.20m^2/s$,

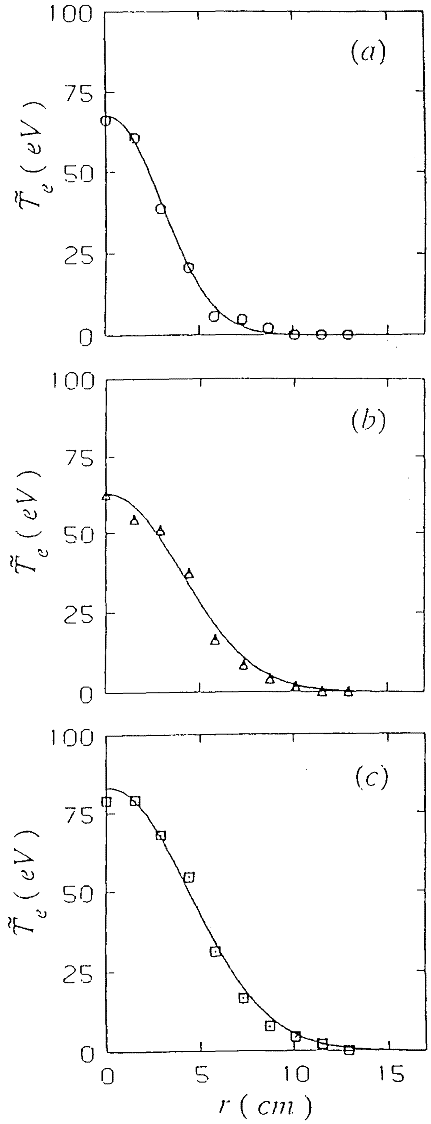


Fig. 5 The temperature perturbation profile at the end of each ECH pulse. These are corresponding to 0.3 ms (a), 0.5 ms (b) and 0.8 ms (c) in ECH pulse length, respectively.

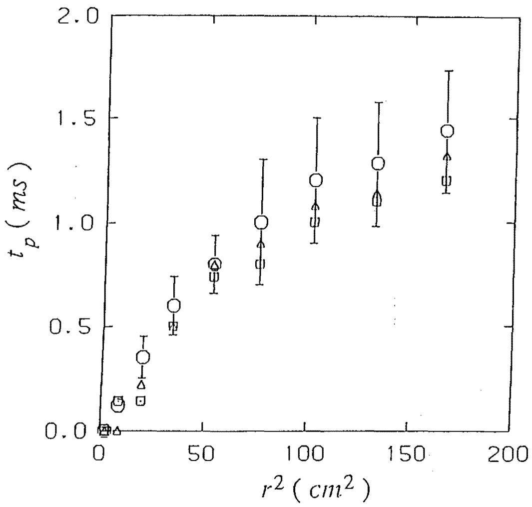


Fig. 6 The experimental time delay ($t_p$) of arrival of the heat pulse peak at differential radii ($r$) (circles : = 0.3 ms, triangles : = 0.5 ms, squares : =0.8 ms) versus $r^2$.

$2.74 \pm 0.77 m^2/s$ corresponding to 0.3 ms (a), 0.5 ms (b) and 0.8 ms (c) in ECH pulse length in Fig. 5. Using the values of $\chi_{HP}$ from the simple time-to-peak method, we calculate the delay time ($t_p$) versus $r^2$. The results are shown in Fig. 7.

We shall consider an approximate solution to Eq. (4-2) obtained by Soler and Callen,[26] assuming that, at least for radii not too large, the electron density $n_e$ and the electron heat conduction coefficient $\chi_e$ can be taken as constant, the convective term and the damping term can be neglected. One has in this case

$$\tilde{T}(r,\ t)=\frac{b^2}{2t}\exp(-b^2r^2/4t)$$

$$\int_0^\infty r'dr'\tilde{T}(r',\ 0)\exp(-b^2r'^2/4t)I_0\left(\frac{b^2rr'}{2t}\right) \tag{4-5}$$

where $b^2=\dfrac{3}{2\chi_e}$ and $I_0$ is the modified Bessel function which is derived in Eq. (2 -7). Introducing the initial condition.

$$\tilde{T}_e(r,\ 0)=A\cdot\exp(-B\cdot r^2) \tag{4-6}$$

(is a reasonably good fit to the experimentally observed $\tilde{T}(r,\ 0)$.), we obtain

$$\tilde{T}(r,\ t)=\frac{Ab^2}{4tB+b^2}\exp(-b^2r^2/4t)$$

$$\sum_{n=0}^{\infty}\frac{1}{n!}\left\{\frac{b^4r^2}{16Bt^2+4b^2t}\right\}^n. \tag{4-7}$$

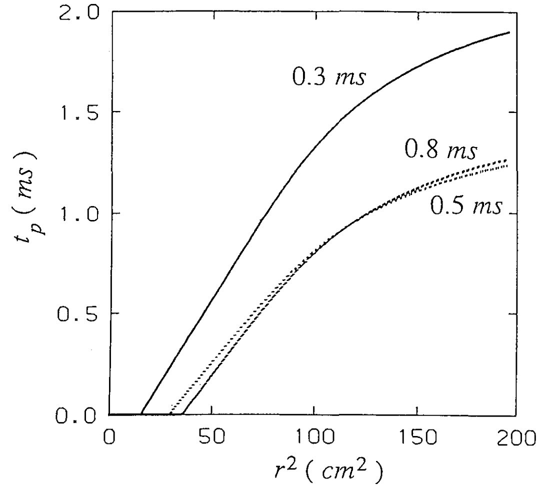


Fig. 7 The time delay ($t_p$) versus $r^2$. Each delay time represent numerical solutions for diffusivc model using the initial temperature perturbation corresponding to Fig. 5. (a), (b) and (c).

Setting $\frac{\partial \tilde{T}(r, t)}{\partial t}$, the relation between $t_p$ and $r_p$ is obtained as

$$t_p = \frac{3\left(r_p^2 - \frac{1}{B}\right)}{8\chi_e}. \tag{4-8}$$

From this simple analysis the value of $r_p$ at $t_p=0$ is $r_p = \frac{1}{\sqrt{B}}$. It indicates that $r_p$ is independent of $\chi_e$. The discrepancy between experimental observation shown in Fig. 6 and numerical calculation shown in Fig. 7 is seen with respect to this value, $r_p(t_p=0)$. This can not be explained by the simple diffusion models for any value of $\chi_e$. The discrepancy may be caused from the neglection of the convective flux in Eq. (4-2) because the damping term can be neglected for this case.

### 3. Re-examination of $\chi_e$ by an introduction of convective flux of heat pulse

Let us consider the equation assuming that $n_e$ and $\chi_e$ are constant values, for simplicity, and the damping term is neglected in Eq. (4-2), i.e.

$$\frac{3}{2} \cdot n_e \cdot \frac{\partial \tilde{T}(r, t)}{\partial t} + \frac{3}{2} \cdot n_e \cdot v_r \cdot \frac{\partial \tilde{T}(r, t)}{\partial r} = \frac{1}{r} \cdot \frac{\partial}{\partial r}\left[ r \cdot n_e \cdot \chi_e \cdot \frac{\partial \tilde{T}(r, t)}{\partial r} \right]. \tag{4-9}$$

In this approach, $v_r$ is an effective convective velocity of the heat pulse which represents a radially averaged effect of all contributions including the small

Table 5 The values of $\chi_e$ and $v_r$.

| ECH pulse length(ms) | $\chi_e(m^2/s)$ | $v_r(m/s)$ |
|---|---|---|
| 0.3 | 6.7 | $1.9 \times 10^2$ |
| 0.5 | 7.0 | $1.9 \times 10^2$ |
| 0.8 | 7.1 | $1.9 \times 10^2$ |

damping effects and the effects of the off-diagonal term in transport matrix. Hence, $v_r$ can not be directly interpreted as the convective velocity. Equation (4-9) can be solved numerically with Dirichlet boundary condition and two free parameters, $\chi_e$ and $v_r$, can be determined by fitting the experimental results in Fig. 6 using the least square fit. The values of $\chi_e$ and $v_r$ corresponding to 0.3 ms (a), 0.5 ms (b) and 0.8 ms (c) in ECH pulse length are shown in Table 5.

In Fig. 9, the solid line represents the best fitted numerical solution of Eq. (4-9) for the experimental results corresponding to 0.5 ms in ECH pulse length. The dotted line represents the numerical solution for diffusive model using the constant value of $\chi_e$ obtained from simple time-to-peak method. It is clearly shown that the discrepancy between numerical simulations and experimental

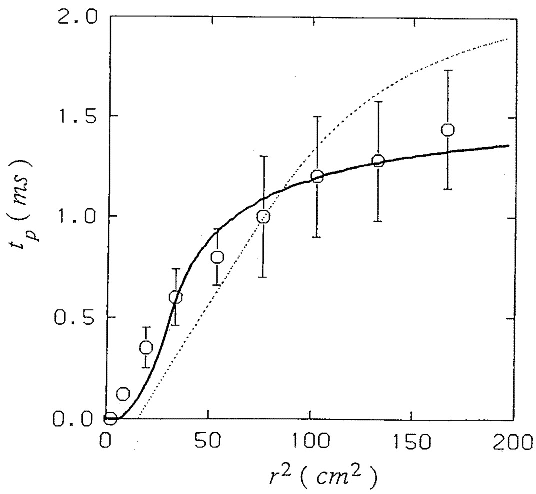


Fig. 8 The solid line represents the best fitted numerical solution of Eq. (4-9) for the experimental results corresponding to 0.3 ms in ECH pulse length. The dotted line represents the numerical solution for diffusive model using the value of $\chi_e$ obtained from simple time-to-peak method.

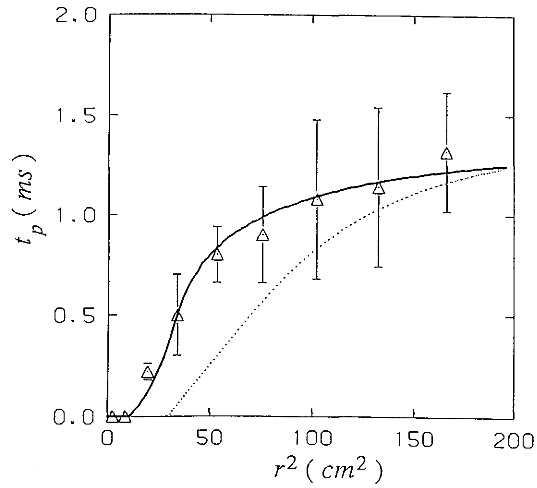


Fig. 9 The solid represents the best fitted numerical solution of Eq. (4-9) for the experimental results corresponding to 0.5 ms in ECH pulse length. The dotted line represents the numerical solution for diffusive model using value of $\chi_e$ obtained from simple time-to-peak method.

results can be resolved by an introduction of the convective term.

## V. Summary and discussion

In summary, we studied the heat pulse propagation problems analytically and numerically. We first focused to the problem of the discrepancy between the $\chi_e$ values derived from heat pulse propagation ($\chi_{HP}$) and those obtained from the stationary power balance ($\chi_{PB}$) observed in the experiments. It has been shown in references[7)8)] that $\chi_{HP}$ can significantly exceed $\chi_{PB}$ if $\chi_{PB}$ is an increasing function of $\nabla T_e$, and that such a dependence is consistent with global confinement properties. The question whether the thermal conductivity has a linear or non-linear dependence on the temperature or temperature gradient was examined by heat pulse propagation analysis. We next applied the heat pulse propagation analysis to the actual experimental data and the comparison studies were made. The possibility that the electron temperature perturbation equation including the convective term could explain experimental observations was also examined by the numerical analysis.

In Chap. II, we reviewed the method to obtain simple estimates of the $\chi_e$ value from the analysis of heat pulse propagation and experimental observations. The ratio of electron heat diffusivity $\chi_{HP}$ to $\chi_{PB}$, as deduced from standard power balance analysis, was considered. If we apply the obtained simple estimation of

$\chi = \frac{r^2}{8t_p}$, it was shown that we can directly obtain $\chi_e$ value from plotting the experimental time delay ($t_p$) of arrival of the heat pulse peak at differential radii ($r$) versus $r^2$. The experimental observations were shown that, basically, in all cases $\chi_{HP}$ is above the corresponding $\chi_{PB}$ typically by a factor of 3.

In Chap. III, heat pulse propagation was analyzed for different models of electron heat conduction coefficient $\chi_e$.[27] Five models were adopted which had various dependence on temperature or temperature gradient. Among them $\chi_e$ having a positive temperature gradient dependence explained the discrepancy between $\chi_{HP}$ and $\chi_{PB}$ observed in the experiments. In this case the deviation was found and shown to have appreciable radial dependence. Two cases that initial temperature perturbation was induced by (1) electron cyclotron heating (ECH) or (2) sawtooth were studied and the results were shown in Table 3 and Table 4. Both Table 3 and Table 4 indicate that $\chi_e$ having a dependence on the temperature gradient is not inconsistent with values of $\chi_{HP}/\chi_{PB}$ obtained from experiments ($\chi_{HP}/\chi_{PB} > 2$). There were preliminary indications to understand the reason for the experimental disagreement between $\chi_{HP}$ and $\chi_{PB}$ which suggested that either this is a feature of observing only high-energy electrons, or that the pulse transport is influenced by the internal disruption mechanism itself. However, the results in Table 3 and Table 4 were obtained without introducing such mechanisms. The value of $\chi_{HP}$ is enhanced by various effects neglected in this numerical calculation (which are high-energy electron, coupling heat flow and plasma diffusion, the internal disruption mechanism, etc). Hence, the results obtained in Table 3 and Table 4 may give the minimum values for $\chi_{HP}/\chi_{PB}$.

In chap. IV, the problem of deducing $\chi_e$ from heat pulse propagation measurements was addressed.[28] For sawtooth free plasma, the local thermal diffusivity was derived with the assumption that the evolution of the temperature profile was governed by a diffusive process in the all confinement region. Comparison study of the experimental observations with the simulations was done, assuming the diffusive process on the propagation of heat pulse induced by local electron heating. It was found that the evolution of electron temperature can not be explained only by simple diffusive models and that an introduction of convective flux term can resolve the discrepancy. From this analysis, we can not conclude anything about the bulk convective velocity $\bar{v}_r$. Chap. III shows that we can not neglect the $\tilde{\chi}$-effect, if $\chi_e$ has a dependence on temperature or temperature gradient. In this analysis, for simplicity, we assume that $\chi_e$ is constant. Hence, it is difficult to compare $v_r$ with $\bar{v}_r$ directly because $v_r$ includes the $\tilde{\chi}$-effect. The radial dependence of the convective flux $v_r(r)$, which is consistent to the $\chi_e(r)$ model, is left for our future work.

**Acknowledgements**

The authors would like to acknowledge Drs. K. Itoh, A. Fukuyama and K. Ida for fruitful discussions. Especially, the introduction to the experimental data of

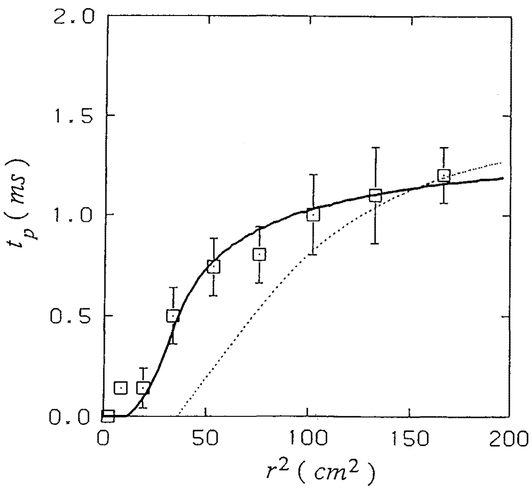


Fig. 10 The solid line represents the best fitted numerical solution of Eq. (4-9) for the experimental results corresponding to 0.8 ms in ECH pulse length. The dotted line represents the numerical solution for diffusive model using the value of $\chi_e$ obtained from simple time-to-peak method.

WT-3 and valuable comments by Dr. K. Hanada are heartily acknowledged.

## References

1. J.D. Callen and G.L. Jahns: Phys. Rev. Lett. **38** (1977) 491.
2. G.L. Jahns, M. Soler, B.V. Waddell, J.D. Callen and H.R. Hicks: Nucl. Fusion **18** (1978) 609.
3. E.D. Fredrickson, J.D. Callen, K. McGuire, J.D. Bell, R.J. Colchin, P.C. Efthimion, K.W. Hill, R. Izzo, D.R. Mikkelsen, D.A. Monticello, V.K. Parē, G. Taylor and M.C. Zarnstorff: Nucl. Fusion **26** (1986) 849.
4. N.J. Lopes Cardozo, B.J.D. Tubbing, F. Tibone and A. Taroni: Nucl. Fusion **28** (1988) 1173.
5. M. Soler and J.D. Callen: Nucl. Fusion **19** (1979) 703.
6. G.L. Jahns, S.K. Wong, R. Prater, S.H. Lin and S. Ejima,: Nucl. Fusion **26** (1986) 226.
7. B.J.D. Tubbing, N.J. Lopes Cardozo and M.J. Van der Wiel: Nucl. Fusion **27** (1987) 1843.
8. K.W. Gentle: Phys. Fluids **31** (1988) 1105.
9. E.D. Fredrickson, K. McGuire, A. Cavallo, R. Budny, A. Janos, D. Monticello, Y. Nagayama, W. Park, G. Tayor and M.C. Zarnstorff: Phys. Rev. Lett. **65** (1990) 2869.
10. N.J. Lopes Cardozo and A.C.C. Sips: Plasma Phys. Controlled Fusion **33** (1991) 1337.

11. Y. Takase, R.J. Goldston, M.G. Bell, A. Cavallo, E.D. Fredrickson, B. Grek, K.W. Hill, D.C. McCune, H.K. Park and J.F. Schivell: Nucl. Fusion **32** (1992) 2246.
12. P.H. Rebut, P.P. Lallia and M.L. Watkins: Plasma Physics and Controlled Nuclear Fusion Research, Proc. 12th Int. Conf. 1988 (Nice) vol II (Vienna: IAEA) p 191.
13. Y.N. Dnestrovskij, S.E. Lysenko, R. Smith: Sov. J. Plasma Phys. **3** (1977) 9.
14. B.B. Kadomtsev: Sov.J. Plasma Phys. **1** (1975) 389.
15. N.J. Lopes Cardozo, J.A. Konings and M. Peters: Nucl. Fusion **32** (1992) 1671.
16. E.D. Fredrickson, J.D. Callen, K. McGuire, J.D. Bell, R.J. Colchin, P.C. Efthimion, K.W. Hill, R. Izzo, D.R. Mikkelsen, D.A. Monticello, V.K. Paré, G. Yaylor and M.C. Zarnstorff: Nucl. Fusion **26** (1986) 849.
17. N.J. Lopes Cardozo, G.M.D. Hogeweij, R.J.E. Jaspers, J.A. Konigs. A.A.M. Oomens, M. Peters, B.C. Schokker, F.C. Schuller, G. Gorinni, P. Mantica, F. De Luca, A. Jacchia, D.J. Barth, F.M.A. Box, D.F. Da Cruz, M. Dircx, A.J.H. Donne, J. F.M. Van Geler, S.H. Heijnen, C.A.J. Hugenholtz, L.C. Ingesson and A.C.A.P. Van Lammeren: Proc. 14th Int. Conf. on Plasma Physics and Controlled Nuclear Fusion Research **1** (1993) 271.
18. T. Maekawa, S. Tanaka, Y. Terumichi, K. Hanada, T. Minami, T. Maehare, K. Makino, Y. Kishigami, T. Kishino and M. Nakamura: Proc. 14th Int. Conf. on Plasma Physics and Controlled Nuclear Fusion Research (Würzburg, 1992) paper IAEA-CN-56/E-3-6-1 (Vienna: IAEA).
19. JET Team: Plasma Phys. Control. Fusion **31** (1989) 1481.
20. L. Laurent: Plasma Phys. Control. Fusion **28** (1986) 85.
21. K.W. Gentle, B. Richards, M.E. Austin, R.V. Bravenc, D.L. Brower, R.F. Gandy, W.L. Li, P.E. Phillips, D.W. Ross, W.L. Rowan, P.M. Schoch, P.M. Valanju and A. J. Wootton: Phys. Rev. Lett. **68** (1992) 2444.
22. K. Itoh, S.-I. Itoh, A. Fukuyama, M. Yagi and M. Azumi: Plasma Phys. Control. Fusion **36** (1994) 279.
23. F. Wagner and U. Stroth: Plasma Phys. Control. Fusion **35** (1993) 1321.
24. W. Goedheer: Nucl. Fusion **26** (1986) 1043.
25. K. Hanada, T. Minami, T. Maehara, K. Makino, Y. Kisigami, T. Kishino, M. Nakamura, T. Maekawa, Y. Terumichi and S. Tanaka: submitted to Plasma Physics and Controlled Fusion.
26. M. Soler and J.D. Callen: Nucl. Fusion **19** (1979) 703.
27. H. Yamaguchi and S.-I. Itoh: J. Phys. Soc. of Jpn. **64** (1995) 1051.
28. H. Yamaguchi, S.-I. Itoh, K. Hanada, T. Kubota and S. Toda: Fusion Tech. **27** (1995) 497.